TECHNOLOGIE 5G

Bulletin de veille scientifique : Mai 2025

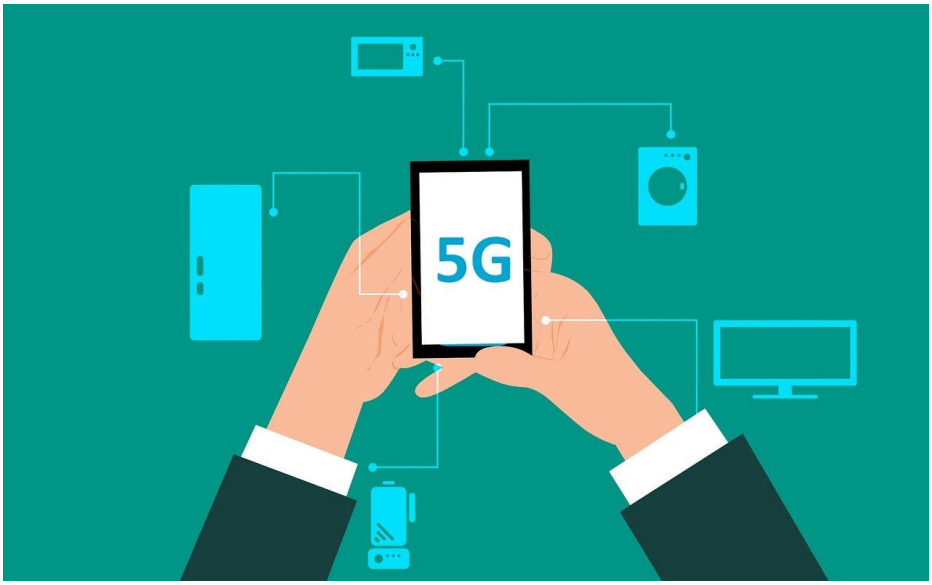

Objectifs : réaliser une veille scientifique sur la technologie 5G

La validation des informations fournies (exactitude, fiabilité, pertinence par rapport aux principes de prévention, etc.) est du ressort des auteurs des articles signalés dans la veille. Les informations ne sont pas le reflet de la position de l'INRS. Les éléments issus de cette veille sont founis sans garantie d'exhaustivité. Les liens mentionnés dans le bulletin donnent accès aux documents sous réserve d'un abonnement à la ressource.

Les bulletins de veille sont disponibles sur le portail documentaire de l'INRS. L'abonnement permet de recevoir une alerte mail lors de la publication d'un nouveau bulletin (bouton « M'abonner » disponible après connexion à son compte).

Généralités

Aucun article dans ce bulletin.

Performances et sécurité

Performance evaluation on extended neural network localization algorithm on 5 g new radio technology.

R D, Markkandan S, Arjunan VK. *Sci Rep*. 2025 May 2;15(1):15354.

With the rapid growth of fifth-generation (5G) networks, there is an increasing demand for high-precision localisation, achieving which is a major challenge in real-time applications in dynamic and noisy environments. Signal noise and incomplete data, including time difference of arrival (TDoA), angle of arrival (AoA), and frequency of arrival (FoA), often limit traditional methods from achieving improved localization. This research proposes an advanced hybrid localisation method combining Extended Kalman Filter (EKF) and Extended Neural Network (ENN) with HackRF-based software-defined radios (SDRs) to improve the real-time localization in 5G environments. The method achieves a better localization accuracy by using EKF for noise reduction and ENN for localization data fusion and combining FoA, AoA, and TDoA measurements. Experiments using real-time 5G signal data show that the proposed EKF-ENN fusion outperforms the existing methods. It obtains an AoA mean of 0.08 radians (SD = 0.014 rad), a TDoA mean of 0.020 s (SD = 0.003 s), and a FoA mean of 0.49 Hz (SD = 0.09 Hz). Its Mean Squared Error (MSE) of 1.06e(6) and Signal-to-Noise Ratio (SNR) of 11.7 dB show that it attains better performance than existing ones. Its increased localisation accuracy and signal processing efficiency qualifies it for real-time usage in next-generation wireless networks.

Lien vers l'article

Radio frequency interface quality assessment in 4G/5G: Effects of IQ imbalance, phase noise, and nonlinearities on error vector magnitude.

Pyatin I, Boiko J, Kovtun V, Kovtun O. *PLoS One*. 2025;20(5):e0324170.

Modern 4G/5G technologies aim to enhance data speeds, improve communication quality, and enable innovative services such as IoT and augmented reality. However, their efficiency depends on minimizing distortions in the radio frequency (RF) interface, evaluated through Error Vector Magnitude (EVM). Increased EVM leads to packet losses and reduced throughput, making its reduction essential for stable and high-quality networks. This study investigates the impact of RF interface imperfections on EVM in 4G/5G systems. The analysis was conducted using Simulink models of digital communication transmitters and receivers, incorporating in-phase and quadrature (IQ) imbalance, phase noise, power amplifier (PA) nonlinearity, channel noise, and signal-coding scheme characteristics. The QM78207 chipset, integrating key RF components, was used as an example to reflect the complexity and quality requirements of modern RF interfaces. The results show that the maximum allowable EVM for 64-QAM is 8% (-22 dB). Variations in IQ amplitude imbalance (0-3 dB) increased EVM from -32 dB to -15 dB, while IQ phase imbalance (0°-15°) caused an increase from -32 dB to -17 dB, both for SNR = 50 dB. These findings are valuable for optimizing RF interface designs in 4G/5G systems, ensuring enhanced communication quality and supporting the growing demands for advanced services.

Lien vers l'article

Design of a 5G MIMO Mobile Intelligent Terminal Antenna with Metasurface Loading.

Xia H, Fan H, Liu Z, Miao H, Song Z. *Sensors (Basel)*. 2025 May 6;25(9).

To achieve multi-band coverage within limited space, reduce antenna types, and enhance communication capabilities, an eight-unit dual-band 5G MIMO antenna array is proposed based on a monopole structure. The antenna operates in two frequency bands (3.23-4.14 GHz and 4.31-5.3 GHz), covering the n78 and n79 bands for 5G applications. The dual-band and miniaturized design of the antenna elements is achieved through the slotting and branch-loading techniques. The orthogonal placement of corner antenna elements is implemented to reduce coupling and optimize spatial utilization, achieving isolation of over 16 dB between elements. The introduction of a metasurface structure further improved isolation by 2 dB and increased the peak gain of the antenna array to 11.95 dBi. A prototype is fabricated and tested, demonstrating the following performance metrics: isolation exceeding 18 dB, gain ranging from 6 to 12 dBi, envelope correlation coefficient below 0.05, channel capacity greater than 41 bps/Hz, diversity gain of approximately 10 dB, total active reflection coefficient below -24 dB, and radiation efficiency exceeding 72%. These results confirm the superior performance of the proposed antenna design.

Lien vers l'article

A low profile super UWB- MIMO antenna with d-shaped for satellite communications, 5G and beyond applications.

Mohamed HA, Aboualalaa M. *Sci Rep*. 2025 May 5;15(1):15660.

This study presents a new compact single-layer microstrip 4-port super UWB MIMO antenna designed to operate in the frequency range of (2.5-50) GHz, achieving an impressive 320.2% impedance bandwidth. The antenna is based on a unique d-shaped geometry, specially tailored for applications in satellite communication, 5G, and Beyond, covering various bands including S-, C-, 4G LTE, sub-6 GHz, UWB, and X, ka-, k-, and ku- satellite communication bands. This aligns with Europe's efforts to harmonize by designating the 26 GHz band as a pioneer band for 5G. Additionally, 5G millimeter-wave frequencies are increasingly used in Internet of Things (IoT) applications and industrial automation. In the 5G spectrum, the midband (FR1) spans 1 GHz to 7 GHz, while the high band (FR2) covers frequencies from 24 to 52 GHz and smart wearable devices, vehicle radars, satellite communications, and smart 5G remote sensors devices. The antenna system comprises four orthogonally symmetrically placed identical radiating elements, each featuring a d-shaped patch. The metallic ground plane incorporates a curvature with a simple half-circle shape, effectively enhancing the antenna's matched bandwidth by altering the current distribution, consequently affecting the inductance and capacitance within the ground plane. A MIMO structure comprising four elements of the proposed antenna is introduced. Both simulation and experiments of the MIMO system demonstrate the antenna's impressive performance, showcasing an impedance bandwidth of 2.5 to 50 GHz, a whole-working bandwidth isolation exceeding 20 dB, an envelope correlation coefficient (ECC) below 0.013, and a significant increase in diversity gain (DG) of over 9.98 dBi. The antenna exhibits excellent radiation characteristics and a stable gain, making it highly suitable for UWB MIMO system applications.

Lien vers l'article

A frequency and beamwidth reconfigurable antenna based on liquid crystal for 5G millimeter waves.

Chen P, Wang X, Wang D, Gan Z, Yin Y, Zhang H. *Sci Rep*. 2025 May 22;15(1):17822.

In this paper, a novel frequency and beamwidth reconfigurable antenna is proposed. The antenna features a 5-layer vertically stacked structure with the dimensions of [Formula: see text] [Formula: see text], and the layers from top to bottom are the radiating layer, the orientation layer, the liquid crystal (LC) layer, the orientation layer, and the ground layer, and a liquid crystal cavity integrated into the LC layer. An inverted microstrip feed line structure is employed as the bias electrode, and connecting it to a coaxial line side-feed adapter for excitation of the antenna. To investigate the beamwidth reconfigurability, two parasitic dipole structures-all disconnected or connected-are placed on either side of the main radiating element for comparative analysis. Experimental results reveal that the antenna's resonance frequency shifts from 31.78 GHz to 27.1 GHz, providing a frequency reconfigurable range of 14.73%. Notably, this frequency tuning process is minimally influenced by the type of parasitic patch. Additionally, the impedance bandwidth and -3dB beamwidth of the antenna remain largely unaffected by the reconfiguration. Testing the antenna with different parasitic patch structures, the -3dB beamwidth of the antenna expands from [Formula: see text] to [Formula: see text] at [Formula: see text] for the LC, and from [Formula: see text] to [Formula: see text] at [Formula: see text], and the antenna peak gain of 6.04 dBi and 7.58 dBi, separately. These results correspond to a reconfigurable range of 64.75% and 40.89% for the -3dB beamwidth, respectively.

Lien vers l'article

Multi antenna structure assisted by metasurface concept providing circular polarization for 5G millimeter wave applications.

Althuwayb AA, Ali EM, Alibakhshikenari M, Virdee BS, Rashid N, Kaaniche K, et al. *Sci Rep*. 2025 May 21;15(1):17579.

This This paper presents a circularly polarized multi-antenna structure designed for 5G millimeter-wave applications. The structure is based on circular patch radiators, each enhanced with metasurface (MTS) characteristics through the integration of multi-split ring slots. Each radiating element is enclosed within a decoupling wall constructed from a microstrip transmission line, which features both wide (capacitive) and thin (inductive) impedance profiles. The antennas are excited from below using metallic pins, which connect to the radiators through via-holes stemming from coplanar waveguide ports on the ground plane. Experimental results demonstrate a wide bandwidth from 25.6 to 29.7 GHz, corresponding to a fractional bandwidth of 14.82%. Additionally, the antenna exhibits stable radiation patterns, with an average gain of 2.7 dBi and a radiation efficiency of 57%. Using a single radiator configuration, a 3×3 antenna array was implemented. In this design, electromagnetic coupling between adjacent radiators is significantly reduced. The resulting array, measuring $20 \times 20 \times 0.32$ mm(3), achieves excellent performance across a wide frequency range from 24 to 31 GHz, corresponding to a bandwidth of 25.45%. Key metrics include an average isolation between radiating elements exceeding 17 dB and an average gain and radiation efficiency of 9.0 dBi and 91.5%, respectively.

Lien vers l'article

Architecture réseau

Aucun article dans ce bulletin.

Efficacité énergétique

Energy efficient relay selection framework for 5G communication using cognitive radio networks.

Rajavel SE, Devaraj SA, Roobert AA, Kumar OP, Vincent S. *Sci Rep*. 2025 May 4;15(1):15566.

The large bandwidth of 5G wireless networks results in a discontinuous optimal spectrum. This study leverages cognitive radio networks and collaborative spectrum sensing to improve the transmission performance in 5G communication. Energy limitations for each secondary user (SU) and potential errors in secondary transmission within cognitive nodes during cooperative transmissions and spectrum sensing contribute to the dynamic energy efficiency. This paper details an Electronic Energy Relay Selection (EERS) system. The weighted average function determines the optimal relays when the network communication power consumption and spectrum-detection levels are equal. The EERS system examines the correlation between energy efficiency and detection precision. The proposed EERS system surpasses the performance of the compressed sensing collaborative detection (CSCD) system. MATLAB was used to evaluate and compare performance metrics such as weighted energy consumption, number of collaborative SU relays, and probability of missing detection with those of compressed sensing-based collaborative detection.

Lien vers l'article

Autres équipements

A Convolution-Based Coding Metasurface for Wide-Angle Beam Steering for Enhanced 5G Wireless Communications.

Wang J, Chen Y, Wang B, Liu X, Gao J, Xue Q, et al. *Materials (Basel)*. 2025 Apr 23;18(9).

With the rapid development of 5G communication technology, there is an increasing demand for high-performance antennas and beam control technologies, making the development of novel metamaterial structures capable of precise electromagnetic wave manipulation a current research hotspot. This paper presents a coding metasurface specifically designed for 5G communication applications, operating at a frequency of 3.5 GHz. The design employs a unique annular metasurface unit structure capable of achieving both single-beam and dual-beam functionalities. Through convolution operations, precise control over the reflection angle is achieved, with an adjustable range from 51.5° to 17.5° and a resolution of 10°. This design overcomes the inherent limitations of traditional gradient coding methods, providing a comprehensive framework for wide-angle reflection control in metasurface design. The research results demonstrate that the coding metasurface can effectively control the reflection direction of electromagnetic waves at 3.5 GHz, exhibiting dual-polarization modulation capabilities and maintaining stable performance under oblique incidence conditions within 20°. Experimental validation confirms the beam control functionality of the design in real-world environments, highlighting its potential to enhance signal reception sensitivity and

transmission efficiency in 5G wireless communications. This work opens new avenues for research in reconfigurable and intelligent metasurfaces, with potential applications extending beyond 5G to future 6G networks and Internet of Things (IoT) systems.

Lien vers l'article

Advancing inorganic electro-optical materials for 5 G communications: from fundamental mechanisms to future perspectives.

Wang H, Chen L, Wu Y, Li S, Zhu G, Liao W, et al. *Light Sci Appl*. 2025 May 12;14(1):190.

In the 5 G era, the demand for high-capacity and fast fiber-optic communication underscores the importance of inorganic optical materials with high electro-optical (EO) coefficients, rapid responses, and stability for efficient electro-optical modulators. The exploration of novel EO materials and their applications remains in the early stages. At present, research mainly focuses on the performance of EO materials and devices. However, the EO coefficients of different preparation methods for the same material and different materials vary significantly. Currently, a crucial gap lies in understanding the link between the EO effect and ferroelectric polarization, hindering advancements in ferroelectric material optimization. This article offers a comprehensive insight into the EO effect, initially discussing ferroelectric polarization and its relationship to the phenomenon. It then reviews standard inorganic ABO(3) metal oxide ferroelectric ceramics and thin films, followed by an examination of emerging ferroelectrics such as HfO(2)-based polymorph ferroelectrics and ZnO/AlN-based materials. The article concludes by addressing the challenges in investigating ferroelectric EO mechanisms and provides an outlook on the future of EO material research, including a review of the latest developments in EO effect mechanisms and their optimization for light modulation, as well as an exploration of potential areas for high-performance EO materials research.

Lien vers l'article

Compact dual band crossover for 5G low and mid band applications using a metamaterial branch line coupler.

Shallah AB, Zubir F, Rahim MKA, Jizat NM, Basit A, Yusof KH, et al. *Sci Rep*. 2025 May 26;15(1):18425.

This research paper introduces a compact dual-band crossover designed for the low and mid-band 5G frequencies at 0.7 GHz and 3.5 GHz. The innovative design is achieved by cascading two dual band branch-line couplers (BLCs), which utilize T-shaped transmission lines (TLs) with folded arms and stubs to reduce their overall footprint significantly. Additionally, the integration of metamaterial (MTM) structures, incorporating interdigital capacitor (IDC) unit cells, contributes to an impressive 90% size reduction compared to conventional components. The BLC's and crossover's performances were rigorously evaluated using CST Microwave Studio (CST MWS) simulations. Following successful simulations, the BLC and crossover were fabricated on a Rogers Duroid/RT5880 substrate, characterized by a dielectric constant of 2.2 and a thickness of 0.787 mm. A thorough comparative analysis between the simulated and measured results, alongside similar reported works, signifies the exceptional performance of the proposed BLC and crossover. These findings confirm their suitability for sub-6 GHz 5G frequency spectrum applications.

Lien vers l'article

Applications médicales et industrielles de la 5G

Applications industrielles

Aucun article dans ce bulletin.

Applications médicales

Perioperative anesthesia management of remote 5G robot surgery and precautions for operation team.

Wang X, Liu S, Lei W, Zhao D, Xu L, Feng Z, et al. *J Robot Surg*. 2025 Apr 1;19(1):133.

Remote 5G robot surgery not only improves the accuracy, accessibility and efficiency of surgery, but also promotes the remote sharing and integration of medical resources, effectively avoids the risk of transshipment, reduces the cost of remote medical treatment, and promotes the development of smart medical care. To successfully carry out remote 5G surgery, it is necessary to establish a medical team, and anesthesiologists should not only escort the operation but also find problems in time when accidents occur and coordinate the team for joint treatment. General anesthesia is selected for this kind of operation, and local nerve block is recommended for analgesia. The main feature of anesthesia is that the patient is completely braked during the whole operation, and it is necessary to provide good muscle relaxation and suitable anesthesia sedation depth. In addition, due to the limited operating space of the head, special posture, long-term artificial pneumoperitoneum, the harm of hypothermia, delayed awakening or postoperative delirium, individualized multi-mode analgesia and other problems. The above problems have caused some challenges and difficulties for anesthesiologists.

Lien vers l'article

Correction: Perioperative anesthesia management of remote 5G robot surgery and precautions for operation team.

Wang X, Liu S, Lei W, Zhao D, Xu L, Feng Z, et al. *J Robot Surg*. 2025 May 27;19(1):242.

Lien vers l'article

Evaluation (Mesure des niveaux d'exposition)

Méthodes d'évaluation

Short-Dipole Sensor Response Linearization Through Physics-Informed Neural Networks.

Fasse A, Meyer R, Neufeld E, Haas M, Chavannes N, Kuster N. *Bioelectromagnetics*. 2025 May;46(4):e70010.

Short-dipole diode sensors loaded with highly resistive lines are commonly used to measure the time-averaged square of the high-frequency electromagnetic field amplitude directly. Their precision, simplicity, broadband, high dynamic range capability, and minimal scattering make them ideal for application in the near-field of sources, particularly for demonstrating compliance with exposure limits. However, the usage of these sensors to cover multiple orders of magnitude of field amplitude requires signal-specific linearization of the sensor response. Traditionally, linearization had been performed for each signal or modulation by measurement and, more recently, by simulations based on a calibrated sensor model. These approaches have become prohibitively expensive with the launch of the fifth generation of mobile communication (5G), which added thousands of diverse and complex modulation schemes. In response to these challenges, we first developed an innovative approach to accelerate sensor model simulations with an enhancement of accuracy, which allows us to subsequently establish a data set comprising a large number of probe parameters and signal characteristic configurations. Subsequently, a physics-informed neural network (PINN) was trained with readily accessible signal characteristics to obtain on-the-fly linearization parameters with acceptable uncertainties across the relevant dynamic range. In contrast to traditional artificial intelligence (AI) models that predominantly rely on pattern recognition from precomputed data, our approach ensures that the model captures the intrinsic relationships and system dynamics inherent to the physical phenomena under study. Our AI-based approach achieves an error below 0.4 dB at peak specific absorption rate (SAR) values of up to > 200 W kg -1 . In addition, AI accelerates the determination of linearization parameters by a factor > 34,000 × and reduces storage requirements > 350,000 times, allowing linearization parameters to be computed on site.

Lien vers l'article

Evaluation population générale

5G EMF Exposure at 3.6 GHz in Greece Using Data From Frequency-Selective Monitoring Sensors.

Iakovidis S, Manassas A, Apostolidis C, Samaras T. *Bioelectromagnetics*. 2025 May;46(4):e70008.

The introduction of 5G networks has raised public concerns about potential changes in environmental electromagnetic field (EMF) exposure. This study analyzes continuous monitoring data collected over 2 years (August 2022-October 2024) from 13 frequency-selective monitoring sensors located in Greece's five largest cities. Focusing on the 3.6 GHz band, we evaluated trends and weekly variations in EMF levels. Results indicated a gradual increase in EMF exposure at 3.6 GHz, driven by the growing penetration of 5G infrastructure and devices. Notably, this band exhibited higher maximum-to-median power density ratios compared to other frequency bands, attributable to active antenna systems' characteristics and traffic variations. Applying the ICNIRP 2020 guidelines, we found that 30-min averaged values significantly reduced these variations. All measured EMF levels, including maximum

values, remained well below Greek and international safety limits. These findings, especially the increasing trend identified for the EMF levels, underscore the importance of continuous monitoring networks for assessing EMF exposure to existing and emerging telecommunications networks and ensuring compliance with safety standards.

Lien vers l'article

Risques professionnels

Aucun article dans ce bulletin.

Effets biologiques et sur la santé

In silico

Aucun article dans ce bulletin.

In vitro

5G-exposed human skin cells do not respond with altered gene expression and methylation profiles.

Jyoti J, Gronau I, Cakir E, Hütt MT, Lerchl A, Meyer V. *PNAS Nexus*. 2025 May;4(5):pgaf127.

Due to the ever-increasing wirelessly transmitted data, the development of new transmission standards and higher frequencies in the 5G band is required. Despite basic biophysical considerations that argue against health effects, there is public concern about this technology. Because the skin penetration depth at these frequencies is only 1 mm or less, we exposed fibroblasts and keratinocytes to electromagnetic fields up to ten times the permissible limits, for 2 and 48 h in a fully blinded experimental design. Sham-exposed cells served as negative, and UV-exposed cells as positive controls. Differences in gene expression and methylation due to exposure were small and not higher than expected by chance. These data strongly support the assessment that there is no evidence for exposure-induced damage to human skin cells.

Lien vers l'article

Sur l'animal

Single exposure to near-threshold 5G millimeter wave modifies restraint stress responses in rats.

Matsumoto A, Endo I, Ijima E, Hirata A, Kodera S, Ichiba M, et al. *Environ Health Prev Med*. 2025;30:33.

BACKGROUND: In response to growing concerns about the health effects of quasi-millimeter waves (qMMW) used in 5th-generation wireless systems, conservative whole-body exposure thresholds based on indirect evidence have been proposed. The guidelines define a whole-body average specific absorption rate (WBA-SAR) of 4 W/kg which causes a 1 °C increase in core temperature, as the operational threshold for adverse health effects. To address the lack of direct evidence, we recently reported that a 30-minute exposure to qMMW at 4.6 W/kg resulted in a 1 °C increase in rat core temperature. Here, we further analyzed the near-threshold stress response for the first time, using biological samples from the aforementioned and additional experiments. METHODS: A total of 59 young Sprague-Dawley rats (240-322 g) were exposed to 28 GHz for 40 minutes at WBA-SARs of 0, 3.7, and 7.2 W/kg, under normal (22.5 °C, 45-55% humidity), and heat (32 °C, 70% humidity) conditions. Rats were restrained in acrylic holders for dose control. We repeatedly measured serum and urinary biomarkers of stress response, aggregated the data, and analyzed them using a single statistical mixed model to subtract the effects of sham exposure and between-subject variation. RESULTS: Sham exposure induced stress responses, suggesting an effect of restraint. After the subtraction of the sham exposure effect, 28 GHz appeared to induce stress responses as evidenced by elevated serum-free

corticosterone 1 or 3 days after the exposure, which was more evident in animals with a change in rectal temperature exceeding 1 °C. Urinary-free catecholamines demonstrated an inhibitory property of 28 GHz frequency exposure on the stress response as evidenced by noradrenaline on the day of exposure. Heat exposure enhanced this effect, suggesting a possible role of noradrenaline in heat dissipation by promoting cutaneous blood flow, a notion supported by the correlation between noradrenaline levels and tail surface temperature, a critical organ for heat dissipation. CONCLUSIONS: This study is the first to demonstrate that qMMW whole-body exposure can alter the stress response as indicated by corticosterone and noradrenaline at near-threshold levels. Our findings may provide insight into the biological basis of the whole-body exposure thresholds in the international guidelines.

Lien vers l'article

Effects of radiofrequency electromagnetic field exposure on cancer in laboratory animal studies, a systematic review.

Mevissen M, Ducray A, Ward JM, Kopp-Schneider A, McNamee JP, Wood AW, et al. *Environ Int*. 2025 May;199:109482.

BACKGROUND: More than ten years ago, the World Health Organization's (WHO) International Agency for Research on Cancer (IARC) published a monograph concluding there was limited evidence in experimental animals for carcinogenicity of Radio Frequency Electromagnetic Field (RF EMF). OBJECTIVE: The objective of this review was to systematically evaluate the effects of RF EMF exposure on cancer in experimental animals. METHODS: Eligibility criteria: Based on pre-established Populations, Exposures, Comparators, Outcomes, and Study Type (PECOS) criteria, studies in experimental animals of the following study types were included: chronic cancer bioassays, initiation-(co-)promotion studies, and studies with tumor-prone animals. INFORMATION SOURCES: MEDLINE (PubMed), Science Citation Index Expanded and Emerging Sources Citation Index (Web of Science), and the EMF Portal. Data abstraction and synthesis: Data are publicly available online as interactive visuals with downloadable metadata. We adapted the risk-of-bias (RoB) tool developed by Office of Health Assessment and Translation (OHAT) to include considerations pertinent to the evaluation of RF EMF exposure and cancer bioassays. Study sensitivity was assessed with a tool adopted from the Report on Carcinogens (RoC). We synthesized studies using a narrative approach. Effect size was calculated as the 1% Bayesian Average benchmark dose (BMD) of a respective study when dose-response or a trend was identified (see BMDAnalysisSupplementaryMaterial) (Supplement 1). Evidence Assessment: Certainty of the evidence (CoE) was assessed using the Grading of Recommendations, Assessment, Developing and Evaluations (GRADE) approach, as refined by OHAT. Evidence from chronic cancer bioassays was considered the most directly applicable to evaluation of carcinogenicity. RESULTS: We included 52 studies with 20 chronic bioassays No studies were excluded based on risk of bias concerns. Studies were not considered suitable for meta-analysis due to heterogeneity in study design, species, strain, sex, exposure characteristics, and cancer outcome. No or minimal evidence of RF EMF exposure-related cancer outcomes was found in most systems or organs in any study (these included gastrointestinal/digestive, kidney, mammary gland, urinary, endocrine, musculoskeletal, reproductive, and auditory). For lymphoma (18 studies), with 6 chronic bioassays (1,120 mice, 1,780 rats) inconsistency between two chronic bioassays was not plausibly explainable, and the CoE for lymphoma was rated 'moderate'. For brain tumors (20 studies), including 5 chronic bioassays (1,902 mice, 6,011 rats), an increase in glial cell-derived neoplasms was reported in two chronic bioassays in male rats. The CoE for an increased risk in glioma was judged as high. The BMD analysis was statistically significant for only one study and the BMD was 4.25 (95% CI 2.70, 10.24). For neoplasms of the heart (4 chronic bioassays with 6 experiments), 3 studies were performed in rats (~2,165 animals), and 1 in mice (~720 animals). Based on 2 bioassays, statistically significant increases in malignant schwannomas was judged as high CoE for an increase in heart schwannomas in male rats.

The BMDs from the two positive studies were 1.92 (95 %CI 0.71, 4.15) and 0.177 (95 %CI 0.125, 0.241), respectively. Twelve studies reported neoplasms in the adrenal gland (5 chronic bioassays). The CoE for an increased risk in pheochromocytoma was judged as moderate. None of these findings were dose-dependent when compared to the sham controls. Sixteen studies investigated tumors of the liver with 5 of these being chronic bioassays. The CoE was evaluated as moderate for hepatoblastomas. For neoplasms of the lung (3 chronic bioassays), 8 studies were conducted in rats (~1,296 animals) and 23 studies in mice (~2,800 animals). In one chronic bioassay, a statistically significant positive trend was reported for bronchoalveolar adenoma or carcinoma (combined), which was rated as moderate CoE for an increase in lung neoplasms with some evidence from 2 initiation-(co-)promotion studies. DISCUSSION: Meta-analysis was considered inappropriate due to the heterogeneity in study methods. The GRADE/OHAT CoE framework has not been frequently applied to animal studies and experience to date suggests refinements are needed. We referred to standard methods in environmental health where CoE is framed in the context of strength of the evidence providing positive support for carcinogenicity. High CoE can be interpreted as the true effect is highly likely to be reflected in the apparent relationship. Moderate CoE indicates the true effect may be reflected in the apparent relationship. Cancer bioassays conducted in experimental animals are commonly used to identify potential human carcinogens. We note that the two tumor types with high CoE in animals in this systematic review are the same as those identified with limited evidence in humans by the IARC Working Group. However, even in cases where the animal evidence demonstrates high CoE, the extrapolation of risk from cancer bioassays to humans is particularly complex for RF EMF. Without a better understanding of the mechanism of the carcinogenicity of RF-EMF, the choice of exposure metric for risk extrapolation (whole body versus localized), intensity or cumulative exposure, whether or not a monotonic dose-response holds for carcinogenic effects, and whether SAR is the appropriate dose metric for adverse effects induced by RF-EMF, may be critical. OTHER: This review was partially funded by the WHO radioprotection programme. The protocol for this review was registered in Prospero reg. no. CRD42021265563 and published in Environment International 2022 (Mevissen et al. 2022).

Lien vers l'article

Sur l'homme

Effects of Mobile Electromagnetic Exposure on Brain Oscillations and Cortical Excitability: Scoping Review.

Torkan A, Zoghi M, Foroughimehr N, Yavari A, Jaberzadeh S. *Sensors (Basel)*. 2025 Apr 26;25(9).

With the widespread adoption of smartphones, concerns about increased exposure to non-ionizing radiofrequency have emerged. This scoping review examines the effects of mobile phone exposure on neural oscillations and cortical excitability, focusing on both motor and non-motor regions of the cerebral cortex. A scoping review identified seventy-eight studies that involved healthy individuals and employed electroencephalography and only two studies that investigated transcranial magnetic stimulation as primary technical tools. The findings suggest that mobile phone exposure may affect brain oscillations and cortical excitability. However, inconsistencies in experimental methods across studies make it difficult to draw definitive conclusions. Additionally, research on fifth-generation technology, particularly mmWave exposure from next-generation mobile networks, remains limited and needs further exploration. These gaps highlight the need for more in-depth studies on how mobile phone exposure impacts brain function.

Lien vers l'article

Reproduction

Interaction of 5G mid-band and mmWave electromagnetic fields with the murine fetus.

Foroughimehr N, Vilagosh Z, McIntosh R, Wood A, Yavari A. *Environ Res*. 2025 Jun 1;274:121188.

Currently, fifth-generation (5G) systems are deploying in the mid-band (i.e., 3.5 GHz (GHz), with plans for standalone (SA) operation in the high-band (i.e., 26 GHz) soon. The literature reveals a lack of computational studies on flora and fauna. This study aims to address that gap and help validate experimental research on animal exposure to electromagnetic field (EMF). We aim to explore the radiofrequency (RF)-EMF absorbed by mouse fetuses through in silico analysis using the Finite Difference Time Domain (FDTD) technique. We utilize the commercial software XFdtd (Remcom) and conduct simulations at both 3.5 and 26 GHz. The investigation focuses on understanding the penetration depth to comprehend EMF absorption by the fetus. While the study indicates that RF-EMF absorption at 5G high-band frequencies is unlikely to pose significant risks to mouse uteruses and fetuses, there is a clear need for further investigation.

Lien vers l'article

Dispositifs médicaux implantables

Aucun article dans ce bulletin.